COHERENT CURRENT VOLTAGE CHARACTERISTICS OF TRIPLE BARRIER RESONANT TUNNELING DIODES AS IMPROVEMENTS OF STANDARD DOUBLE BARRIER DIODES

U. Merc[1], C. Pacher[2], F. Smole[1], and M. Topič[1]

[1] Faculty of Electrical Engineering, University of Ljubljana, Ljubljana, Slovenia

[2] ARC Seibersdorf research GmbH, Tech Gate Vienna, Wien, Austria

Key words: Resonant tunneling, double barrier diode, triple barrier diode, current voltage characteristic, negative differential resistance

Abstract: In double barrier resonant tunneling diodes (DBRTD) as well as in other small period number structures coherent electron transport dominates the total current through the structure. Since coherent transport is a result of a resonant tunneling phenomenon we can use transmission spectra to derive current density vs. voltage characteristics. The topic of our study is to improve an initial DBRTD by increasing two of the most important parameters of RTDs: peak current density and peak-to-valley ratio (PVR) defining a negative differential resistance region. In order to provide assistance in experimental efforts to design resonant tunneling systems with optimal peaks, both in the transmission spectrum and the current density, we attempt to explore whether the observations seen for the DB diode hold as well for the triple barrier (TB) diode. In this paper we show that by using TBRTDs with an increased barrier height improvements of the initial DBRTD structures are possible. We show the influence of broad resonant peaks of an anti-reflection coating in TBRTD structures on the increase of the peak current density. This extra current density can further compensate an increase of the barrier height that increases the PVR and the operating temperature of the structure.

Koherentna tokovno-napetostna karakteristika diode z resonančnim tuneliranjem s tremi barierami kot izboljšava standardne diode z dvema barierama

Ključne besede: Resonančno tuneliranje, dioda z dvema barierama, dioda s tremi barierami, tokovno-napetostna karakteristika, negativna diferencialna upornost

Izvleček: V strukturah z dvema barierama (DBRTD – Double Barrier Resonant Tunneling Diode) kakor tudi v ostalih strukturah z majhnim številom period, katerih osnovni način delovanja temelji na principu resonančnega tuneliranja, prevladuje koherenten način transporta elektronov po strukturi. Ker je koherentni transport plod fenomena resonančnega tuneliranja, lahko na osnovi prepustnostnega spektra strukture določimo odvisnost tokove gostote od napetosti. Predmet naše raziskave je izboljšati lastnosti neke začetne DBRT diode tako, da povečamo dva najpomembnejša parametra diod z resonančnim tuneliranjem: vrhnjo tokovo gostoto in razmerje med vrhnjo in dolinsko vrednostjo tokove gostote (PVR – Peak-to-Valley Ratio). Oba parametra v največji meri določata območje negativne diferencialne upornosti. Z namenom zagotavljanja pomoči eksperimentalnim naporom pri načrtovanju sistemov z resonančnim tuneliranjem, ki bi imeli optimalne vrhove tako v prepustnostnem spektru kot vrhove tokove gostote, smo poskušali raziskati, ali lastnosti DB diod veljajo tudi za diode s tremi barierami (TB). V tem delu predstavljamo, da lahko z uporabo TBRT diod s povišanimi barierami izboljšamo lastnosti začetne DBRT diode. Prikazujemo vpliv širokih resonančnih vrhov TBRT diode s protiodbojno zaščito na povečanje vrhnje tokove gostote, ki omogoči povečanje višine barier ter s tem PVR-ja. Diode z višjimi barierami pa lahko delujejo pri višjih temperaturah.

1. Introduction

Despite the fact that approximately 30 years have passed since the pioneering theoretical and experimental work on resonant tunneling in semiconductor heterostructures by Esaki, Chang, and Tsu /1, 2/, there is still a significant amount of research in this field, which is being sparked by new technical advances in the nanofabrication of these semiconductor heterostructures /3/ and the potential exploitation of the physics of resonant tunneling in producing solid-state devices.

The basic resonant tunneling diode (RTD) device configuration is a double barrier (DB) heterostructure of nanometer dimensions, including two heavily doped semiconductor contact layers to provide low-resistance made from a degenerate *n*-type semiconductor with a relatively small bandgap, e.g. GaAs, (Fig. 1a). These layers comprise the emitter and collector region on both sides of the DB, respectively. Barriers are made from a semiconductor with a relatively large bandgap, e.g. $Al_xGa_{1-x}As$, and in particular a positive conduction-band offset E_B with respect to the smaller bandgap semiconductor. Between the two barriers is the quantum well made again from the smaller bandgap semiconductor. The structure is explained in terms of a conduction-band energy diagram since we are interested in the electron transport process. Because the characteristic dimensions of the DB structure are comparable with the electron wavelengths, the wave nature of electrons leads to quantum phenomena such as interference, tunneling, energy quantization, etc. /4/. As a result, resonant tunneling phenomena occur and form the basis of RTD operation.

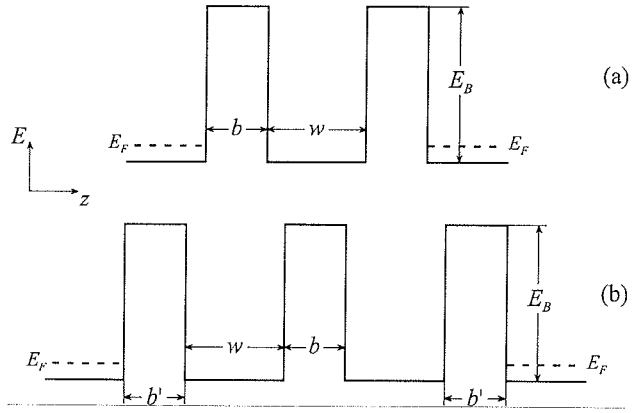

Figure 1: Conduction-energy-band diagram of (a) DBRT and (b) TBRT structure. b *and* w *denotes the barrier and well width, respectively, while* E_B *is the barrier height. For the emitter and collector region Fermi energy* E_F *is shown. In (b)* b' *denotes the outermost barriers width.* z *is spatial coordinate.*

While much of the initial research efforts lie in understanding the physics of resonant tunneling in DB structures, there has been increased experimental /5/ and theoretical /6/ research on resonant tunneling in triple-barrier (TB) semiconductor heterostructures (Fig. 1b). The physics of resonant tunneling in these systems is much more than an extension of the results of the DB case, since it involves the coupling of quasibound states between the two adjacent quantum wells in the semiconductor heterostructure /7, 8/. In particular, while there have been a number of theoretical calculations on the physics of resonant tunneling in DB semiconductor heterostructures in an effort to understand the experimental results /1, 2, 9/, there has been very little theoretical work on systematic understanding of the effects of non-equality of barriers and wells (width and height, respectively) in TB systems /10/. We show that a colorful range of the transmission spectra and corresponding current densities of different TB structures can be constructed. Performed calculations attempt to explore whether the observations seen for the DB diode also hold for the TB diode, while providing theoretical assistance in experimental efforts to design resonant tunneling systems with optimal peaks, both in the transmission spectrum and current-voltage characteristic, respectively.

In this paper we study electron transport by using a coherent model /4, 11, 12/, where particles maintain their phase coherence across the whole structure before losing energy in the contacts (transversal energy and phase coherence during the tunneling process are conserved). As a further approximation we assume that the contacts are perfectly absorbing. This means that when a particle injected from one side reaches the contact region of the other side its phase coherence and excess energy are lost through inelastic collisions with the Fermi sea of electrons in the contact. Thus we assume that an electron injected from one contact at a certain energy E has a certain probability $T(E)$ of being transmitted through the barriers, exits with the same energy and transverse momentum, and finally is absorbed in the opposite contact, where it loses the energy and memory of its previous state. In coherent models electronic conduction in quantum systems is represented by the Landauer and Büttiker /13, 14/ formulation based on the transmission coefficient $T(E_z)$. In this work we use a scattering matrix model /11/ to calculate $T(E_z)$. The transmission $T(E_z)$ as a function of the longitudinal electron energy is the probability ratio of transmitted and incident waves of a particular electron state, which is equivalent to the ratio of the transmitted and incident electron flux. $T(E_z)$ can be calculated from the wave functions available in the solution of the Schrödinger equation. Current flow in this picture is essentially the net difference between the number of particles per unit time transmitted to the right and those transmitted to the left. The current density can be evaluated using the Tsu-Esaki formula /2/ that is obtained by summing the current density of each state over the occupied states multiplied by their transmission probability:

$$J_{total} = \frac{qm^* k_B T}{2\pi^2 \hbar^3} \int_{E_C}^{\infty} T(E_z) \cdot \ln\left(\frac{1+\exp\left(\frac{E_F - E_z}{k_B T}\right)}{1+\exp\left(\frac{E_F - E_z - qV}{k_B T}\right)} \right) dE_z, \quad (1)$$

where q is elementary charge, m^* effective mass, k_B Boltzmann's constant, T temperature, $\hbar$ Planck's constant/2π, E_F Fermi energy, E_z electron's energy in the longitudinal direction, V applied bias, and E_C bottom of the conduction band. The logarithmic term is sometimes called a supply function /15/, since it more or less determines the relative weight of available carriers at a given perpendicular energy and is obtained by integrating over the transverse momentum. This results in a three-dimensional treatment of electron states. In our model space-charge effects are not considered.

In real devices the difference between the measured and calculated results for J_P and PVR can become quite significant, and the voltage range for the occurrence of the Negative Differential Resistance (NDR) does not correspond exactly /16/. Part of the latter problem may be explained by including a series resistance /17/. However, this does not rectify the other discrepancies, particularly the magnitude of J_P which becomes larger than in ideal - coherent - model /16/. The physical processes involved in RTD operation are actually much more complex than the preceding simple description and are especially complicated by the electron's interaction with its environment. The extra valley current represents contributions due to scattering of electrons /18/. Elastic scattering in RTDs may be nominally associated with interface roughness at the heterojunction interfaces, unintentional doping in the tunneling region, impurities, and alloy disorder. Inelastic scattering via phonons and collective excitations do not only break

the assumption of electron energy and transverse momentum conservation but lead also to loss of total phase coherence /11/. The tunneling in both cases can be no longer characterized as coherent, since scattering allows relaxation of the parallel-momentum conservation rule and thus increases the amount of current that may flow off-resonance. Therefore, it can be concluded that the origin of the NDR requires energy and momentum conservation as a condition.

Nevertheless, coherent models representations are in general sufficient to reveal the idea of RTDs operation, especially when small period (barrier + well) number structures /7, 10/ with thin wells and barriers are considered, sometimes when symmetric structures are studied /19/, and in all structures where the mean free path of the electrons is larger than the dimensions of the RT structure (long scattering times) /19, 20/. In these cases scattering can be neglected and coherent models may be applied /8, 20/.

2. DBRT Diodes

Let us start with two DBRT diodes comprised of GaAs/$Al_xGa_{1-x}As$ layers, where the Al composition x was equal to 0.30 and 0.45, respectively. The conduction band offset (barrier height E_B) for those materials is equal to 0.288 and 0.432 eV, while the widths of one well w (GaAs) and two barriers b ($Al_xGa_{1-x}As$) were chosen to be 3.0 and 3.5 nm, respectively. To account for non-parabolicity due to the multiband effects present in the structures /21/ we included in our numerical model energy dependent effective masses $m_{b/w}(E)$ /22/. The temperature and the difference between the Fermi energy and the bottom of conduction band in a degenerate semiconductor were set to 4.2 K (temperature of liquid helium) and 46 meV, respectively. Throughout this work present set of parameters is used unless specified differently.

As seen in Fig. 2, with a positive bias applied to the collector relative to the emitter (contact emitting electrons), the resonant energy level in the quantum well (E_1) approaches the Fermi energy in the emitter increasing the number of electrons that can tunnel. By increasing the bias, the Fermi energy passes through the resonant state making a large current flow due to the increased transmission from the emitter to the collector. At the same time, the back flow of carriers from the collector to the emitter is suppressed as electrons at the Fermi energy in the collector see only a large potential barrier. At a point where the resonant energy aligns with the bottom of the emitter conduction band (Fig. 2b) the number of tunneling electrons per unit area reaches a maximum. Further bias pushes the resonant level under the bottom of the emitter conduction band (Fig. 2c) and cuts-off the electrons coherently tunneling through this resonant state. The supply of electrons is than cut-off. The tunneling current density has therefore a sharp drop from its peak value giving rise to a pronounced region of NDR. A further increase of the bias enables the enhancement of tunneling through higher resonant levels increasing the number of current density peaks. Those current peaks are much higher and wider due to much broader resonant peaks (RPs), which broaden with increasing energy and/or bias. For that reason, the NDR region can become very small. In real devices where scattering is present the NDR region for higher resonant peaks is rarely observed /16/. The current peaks are additionally affected by an increasing temperature that lifts up the electron distribution in the emitter and leads to an increased electron thermionic emission and tunneling through and above the top regions of the barriers /23/. Therefore, we concentrated our study around the first current peak followed by the first NDR region. This is where RTDs are usually used /16, 24/.

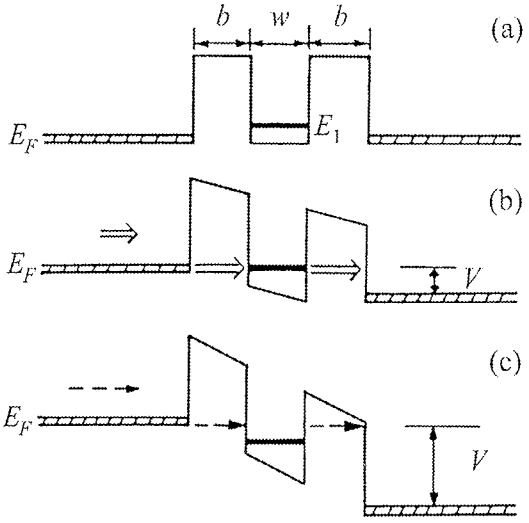

Figure 2: Conduction-energy-band diagram of DBRT structure with three different applied biases.

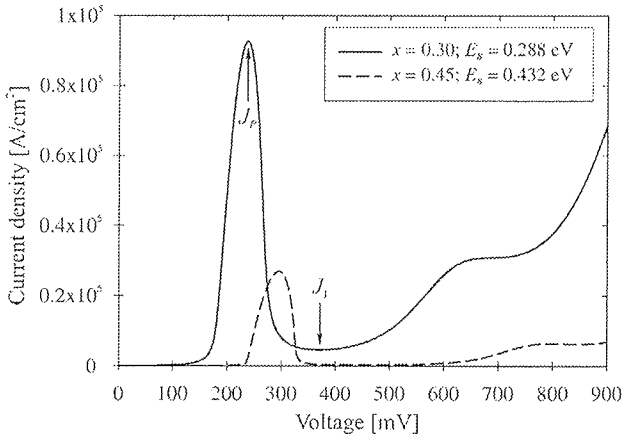

Figure 3: Calculated coherent J(V) characteristics of DBRTD (w = 3 nm and b = 3.5 nm) with Al composition x = 0.30 (E_B = 0.288 eV) and x = 0.45 (E_B = 0.432 eV) at T = 4.2 K are shown by solid and dotted line, respectively.

In Fig. 3 we show the calculated current density vs. voltage characteristics for two DBRTDs with different Al compositions (x = 0.30 and x = 0.45) at T = 4.2 K. We can see that the higher the barriers the smaller the peak current density J_P and the higher the Peak-to-Valley Ratio [PVR = J_P/J_V, where J_V is the valley current density (the minimum current density following J_P by increasing the voltage)] (Table 1). The reasons can be found in the transmission spectrum (TS) of the structures. They show that higher barriers (HB) lead to sharper resonant peaks, although the number of resonant peaks in the quantum well is increased /12/. For most applications /24/, NDR devices such as RTDs should exhibit high J_P and PVR. They both depend physically on the Fermi energy in the emitter and hence the doping there as well as on the temperature /12, 23/. By increasing either of them J_P would increase, while the PVR would decrease until the NDR effect would completely vanish. The reason is in an increase of the resonant tunneling current through higher energy levels, non-resonant currents between the resonant levels, and thermionic emission over the barriers /12/.

For RTDs basically three parameters are important: J_P, PVR, and Voltage Peak-to-Valley Ratio (VPVR) (Table 1). The latter is defined as a ratio between the voltage at J_P (peak voltage V_P) and at J_V (valley voltage V_V) (VPVR = V_P/V_V,). Therefore, the higher the VPVR (approaching toward unity) the steeper the NDR region (with respect to the PVR). A high VPVR is very important for fast logic circuits /25, 26/.

Table 1: J_P, PVR, V_P, and VPVR of DBRTDs from Fig. 3.

x	J_P [10^5 A/cm^2]	PVR	V_P [mV]	VPVR
0.30	0.93	20.18	238	0.64
0.45	0.27	96.20	296	0.67

By using the coherent model we studied different TBRTDs and compared them to DBRTDs. Our main goal was to find a structure, either with two or three barriers, where at the same time the J_P and the PVR would be higher than in the initial (first considered) DBRTD. If possible, in the real device scattering mechanisms should be reduced also compared to the initial DBRTD.

3. TBRT diodes

By studying the coherent picture of TBRTDs the operating principles of DBRTD can be followed. Usually, TBRTDs are used for generating multiple NDR characteristics for multiple-valued logic circuits /25, 26/. In our study the TBRTDs were used in order to improve the coherent $J(V)$ characteristic of the DBRTDs. The novel idea was to vary the width of the two outermost barriers b' of TBRTD structures (Fig. 1b).

In coherent models most of the physical behavior is represented by the transmission spectrum. Fig. 4 shows the transmission spectrum of GaAs/$Al_{0.3}Ga_{0.7}As$ TBRTDs, where the outermost barriers width b' is varied from 0.4 to 4 nm. From the figure it is evident that for thicker outermost barrier widths there are two resonant peaks with a transmission probability equal to unity. As b' decreases, the two peaks forming a quasi-miniband gain stronger coupling. This means that the peaks lie closer to each other, while the valley value between them increases. At a point where b' becomes equal to one half of the central barrier width ($b' = b/2$ - in our case 1.75 nm) both peaks join and form a single resonant peak with a transmission probability equal to unity. Such a b' was presented as an Anti-Reflection Coating (ARC) /27/. We name the whole structure "ARC-TBRTD". By further decreasing b', the two resonant peaks coupled in one peak start loosing their high transmission probability as well as their sharpness (loosing Lorentzian line-shape /28/).

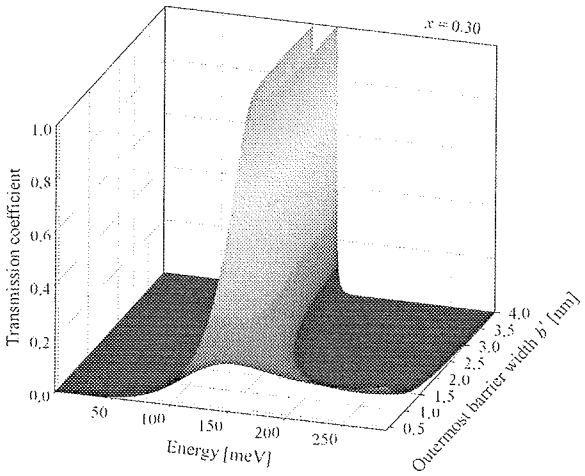

Figure 4: Transmission spectrum for GaAs/$Al_{0.3}Ga_{0.7}As$ TBRTDs with w = 3 nm, b = 3.5 nm *and* b' *varies from 0.4 to 4 nm (no applied bias).*

Another very important parameter for studying TBRTDs is the area under the resonant peaks. In Fig. 5 the area is shown for the structures in Fig. 4 (the area is taken between the energies where the transmission coefficient equals 15%). For real device applications the structure should exhibit the highest J_P with respect to as high PVR as possible. Since a high area under the resonant peaks results in a high J_P, the ARC structures with the highest area are one of the most promising structures. Beside that, the ARC structures can have a relatively high PVR. The reasons lie in the TS. In the ARC structure two coupled resonant peaks form one resonant peak that is much broader than the single resonant peak of the DBRTD, while it is still very steep and has a high transmission probability (Fig. 4). This has many effects on $J(V)$ characteristics of real devices. First of all, the structures can operate at higher temperatures while still exhibiting an NDR region [for x = 0.30 structures, going from 4.2 to 300 K, the PVR of the ordinary ($b' = b$ = 3.5 nm) TBRT device decreases by 57%, while for the ARC-TBRTD ($b' = b/2$ = 1.75 nm) it

decreases for only 9%; the PVR of the DBRT decreases by 63%] /23/. Next, since elastic scattering additionally broadens the resonant peaks in the TS, real devices with broader peaks are relatively less affected by the scattering /12/. For this reason, the operating temperature of the ARC-TBRTD devices can be further increased. In the contrary, for outermost barrier widths smaller than $b/2$, the shape of the resonant peaks (Fig. 4) changes in a way that non-resonant currents are increased (currents not passing through the resonant peaks). The structures can be therefore used only at low temperatures /23/. Finally, b' of the structure should not be too small in order to maintain a steep NDR region (Fig. 6).

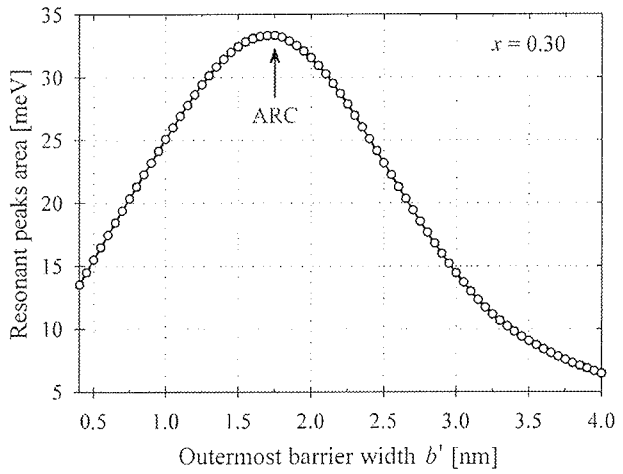

Figure 5: Area of resonant peaks from Fig. 4 vs. b' at zero bias.

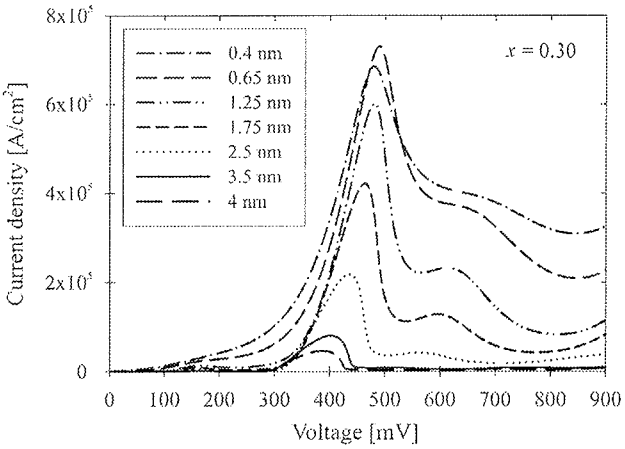

Figure 6: Calculated coherent J(V) characteristics of GaAs/Al$_{0.3}$Ga$_{0.7}$As TBRTDs with w = 3 nm, b = 3.5 nm and b' between 0.4 and 4 nm (T = 4.2 K).

In Fig. 6 we show coherent $J(V)$ characteristics of TBRT diodes with different b'. It is evident that as b' decreases the NDR region gets less pronounced, making the structures less interesting as RTD devices /29/ (Table 2).

Table 2: J_P, PVR, V_P, and VPVR of TBRTDs from Fig. 6.

b' [nm]	J_P [10^5 A/cm^2]	PVR	V_P [mV]	VPVR
0.4	6.85	2.22	480	0.57
0.65	7.30	3.49	488	0.58
1.25	6.00	2.71	480	0.85
1.75	4.22	3.76	464	0.86
2.5	2.18	6.14	436	0.86
3.5	0.80	10.32	402	0.85
4	0.46	12.49	388	0.84

Since the VPVR of the DBRTD that we use in our study as an initial device is not a critical parameter (0.64 for x = 0.3 and 0.67 for x = 0.45) and can be easily obtained with TBRTDs, our detailed analyses concentrate on J_P and PVR, respectively (Fig. 7).

From the study of J_P in Fig. 7a it can be concluded that by changing b' the current density peak varies. By decreasing b' the J_P increases until it reaches a maximum and starts decreasing. For small temperatures /23/ (like in our case where T = 4.2 K) the maximum J_P is not necessarily achieved for the ARC structure (Fig. 7a). This is due to the splitting of the coupled resonant peaks, although the area of the peaks for zero field has a maximum there (Fig. 5). The same holds for the PVR /23/. From Fig. 7b it is evident that by decreasing b' the PVR decreases up to a point where it has a sudden and sharp increase, and after which it decreases again. For TBRTD structures with x = 0.30 the increase of the PVR is at approximately b' = 0.85 nm, which means that the best trade-off between the J_P and PVR is not achieved for an ARC structure ($b' = b/2$). By increasing the height of the barriers (in order to maintain a direct semiconductor x must not be higher than 0.45 in the $Al_xGa_{1-x}As$ system) the increase of the PVR shifts to higher b'. Our detailed analyses showed that by increasing x the highest PVR is achieved for $b' \approx b/2$ (in our case b' = 1.75 nm for x = 0.45). This means that also for lower temperatures the ARC structures can exhibit the best trade-off between the J_P and the PVR.

The reason for the sudden increase of the PVR can be again found in the TS. We have already explained that in the TBRTDs the two resonant peaks couple and form single peak. When a bias is applied these coupled peaks start to split. For that reason the $J(V)$ characteristics can exhibit more current peaks with different heights and widths. These peaks shift their position by changing b'. All this has a big influence on the valley currents. They are composed of the resonant currents as well (the calculated coherent characteristics match better to the measured results) /30/. In this way for a range of b' higher PVRs can be achieved.

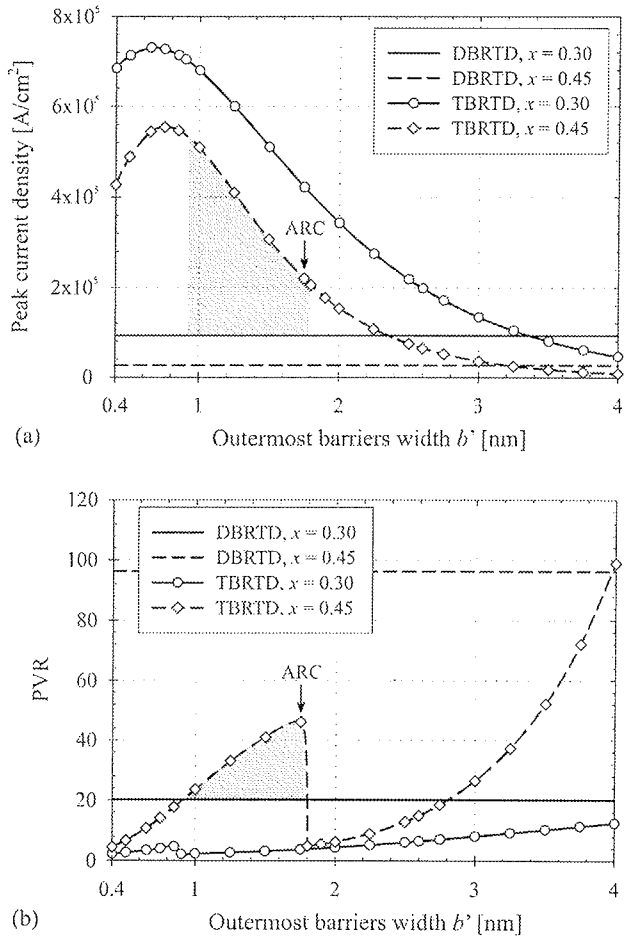

Figure 7: (a) J_P and (b) PVR vs. b'. In both plots the horizontal lines show values of the DBRTDs with different Al composition (different E_B), while symbols connected with an eye-guide line represent the values calculated for the TBRTDs (again for two different E_B). Gray shaded areas show the outermost barrier widths region (0.9 nm < b' < 1.75 nm), where the TBRTDs with x = 0.45 exhibit an improved characteristics with respect to the DBRTD with x = 0.3. (T = 4.2 K)

4. Comparison of structures

Consider the DBRTD with $x = 0.3$ (solid horizontal line in Fig. 7a and b) as an initial structure and compare it to the TBRTDs with different b' and $x = 0.3$ as possible improvements (circles in Fig. 7 connected with a solid eye-guide line). We can see that for $b' < 3.35$ nm the J_P of the TBRTD is higher than 93 kA/cm^2 but the PVR is in the whole studied range smaller than 20.18 (values of J_P and PVR are for the DBRTD - Table 1). The same is for higher b', where the PVR of the TBRTDs becomes higher than in the DBRTD (not shown in the Fig. 6) but the J_P becomes smaller. Therefore, it can be concluded that from a coherent point of view by changing only b' of the TBRTDs it is not possible to construct a structure that would exhibit higher J_P and PVR (at the same time) as they are in the DBRTD with the same b, w, and E_B.

In order to find a structure with improved $J(V)$ characteristics we increased the barrier height. The dashed horizontal lines in Fig. 7 show J_P and PVR of the DBRTD with $x = 0.45$ (Table 1). While the PVR of the latter structure equals 96.20 and is much higher than in the DBRTD with $x = 0.3$ this is not true for the J_P, which is now only 27 kA/cm^2. So again, the DBRTD with $x = 0.3$ cannot be improved by increasing E_B alone.

Finally, we increased E_B of the TBRTDs ($x = 0.45$) (diamonds in Fig. 7 connected with a broken eye-guide lines). It can be seen that the peak current densities decrease and the PVRs increase (a linearly increasing E_B results in a linearly decreasing J_P and an exponentially increasing PVR. This makes structures with higher barriers more interesting as devices /23/). The results of the comparison show again that no TBRTD with $x = 0.45$ has higher J_P and PVR at the same time than the DBRTD with $x = 0.45$. But on the other hand, a comparison between the TBRTDs with $x = 0.45$ and the initial DBRTD with $x = 0.3$ shows that for b' between 0.9 nm and 1.75 nm the J_P as well as the PVR are higher. Only in this way we have at the same time managed to increase the J_P and the PVR of the DBRTD with $x = 0.3$ by using the ARC-TBRTD with $x = 0.45$ from 93 kA/cm^2 and 20.18 to 220 kA/cm^2 and 46.22, respectively.

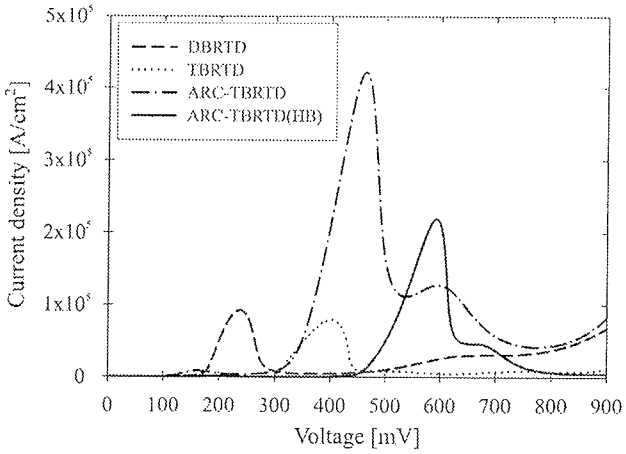

Figure 8: Calculated coherent J(V) characteristics of DBRTD, TBRTD, and ARC-TBRTD all with x = 0.3, and ARC-TBRTD with x = 0.45 (HB); T = 4.2 K.

Fig. 8 shows the final comparison of the coherent $J(V)$ characteristics between the initial DBRTD with $x = 0.3$ and the different TBRTDs that were studied in order to find an improved RTD [TBRTD and ARC-TBRTD both with $x = 0.3$, and ARC-TBRTD(HB) with $x = 0.45$]. It can be seen that for all TB structures the current density peak emerges at higher biases than for the DB structure and that for the structure with higher barriers the peak lies at even some additional bias. It is important to note that all TBRTDs ex-

hibit steeper NDR region than the DBRTD, which is advantageous in fast logic circuits /29/.

Our quest to find an improved structure treated many RTDs with different well and barrier widths. The results show that an improvement of $J(V)$ characteristics is possible only for structures where the barrier width slightly exceeds or is approximately equal to the well width.

5. Conclusions

The most important parameters of RTDs are a high J_P and a high PVR. Both are usually predefined by the device specifications and are especially hard to meet at higher temperatures (200 K and more). The key idea of this paper is how to use TBRTDs in order to improve the coherent $J(V)$ characteristics of DBRTDs. For that reason we have studied different double and triple barrier structures by means of coherent modeling approach, which is applicable for low temperatures. From our analyses it can be concluded that the coherent current-voltage characteristic of the DBRTD cannot be improved only by using the TB structures by itself, nor only by increasing the barrier height. In order to increase both, the J_P and the PVR of the DBRTD, TB structures with different outermost barrier widths and increased barrier height have to be considered.

5. References

/1/ L. Esaki and R. Tsu, *IBM J. Res. Dev.*, V. 14, N. 16, y. 1970; L. L. Chang, L. Esaki, and R. Tsu, *Appl. Phys. Lett.*, **24**, 593 (1974); L. Esaki and L. L. Chang, *Phys. Rev. Lett.*, **33**, 495 (1974); L. Esaki, *Rev. Mod. Phys.*, **46**, 237 (1974); L. L. Chang, *Resonance Tunneling in Semiconductors*, edited by L. L. Chang, E. E. Mendez, and C. Tejedor, Plenum, New York, 1991.

/2/ R. Tsu and L. Esaki, *Appl. Phys. Lett.*, **22**, 562 (1973);

/3/ T. C. L. G. Sollner, et al., *Appl. Phys. Lett.*, V. 43, N. 588, y. 1986.

/4/ S. Datta, *Electronic Transport in Mesoscopic Systems*, Cambridge University Press, Cambridge, 1997, ISBN 0521599431.

/5/ T. Nakagawa, H. Imamoto, T. Kojima, and K. Ohta, *Appl. Phys. Lett.*, V. 49, N. 73, y. 1986; T. Nakagawa, et al., *Appl. Phys. Lett.*, V. 51, N. 445, y. 1987; V. 50, N. 975, y. 1989; D. A. Collins, et al., *Superlatt. Microstruct.*, V. 8, N. 455, y. 1990; E. R. Brown, C. D. Parker, A. R. Calawa, and M. J. Manfra, *Appl. Phys. Lett.*, V. 62, N. 3016, y. 1993.

/6/ X-W Liu and A. P. Stamp, *Phys. Rew. B*, V. 47, N. 16605, y. 1993; H. Yamamoto, Y. Kanie, M. Arakawa, and K. Taniguchi, *Appl. Phys. A*, V. 50, N. 577, y. 1990; H. Yamamoto and Y. Kaine, *Phys. Stats Solidi B*, V. 160, N. K97, y. 1990; J. M. Xu, V. V. Maolv, and L. V. Iogansen, *Phys. Rev. B*, V. 47, N. 7253, y. 1993; Y. Zebda and A. M. Kan'an, *J. Appl. Phys*, V. 72, N. 559, y. 1992.

/7/ H. Yamamoto, K. Tsuji, Y. Ikeda, and K. Taniguchi, *Materials Sci. and Engineering B*, **35**, (1995) 421-428.

/8/ R. Romo, J. Villavicencio, and G. G. Calderon, Phys. Rev. B, **66**, 033108 (2002).

/9/ M. Hirose, M. Morita, and Y. Osaka, Jpn. J. Appl. Phys., V. 16, N. 561, y. 1977.

/10/ X. B. Zhao and H. Yamamoto, Phys. *Stat. Sol. (b)*, **214**, 35 (1999).

/11/ S. Datta, *Modular series on solid state devices - Quantum Phenomena*, Addison-Wesley publishing company, New York, 1989, ISBN 0-201-07956-9.

/12/ D. K. Ferry, *Transport in nanostructures*, Cambridge University Press, Cambridge, 1997, ISBN 0-512-46141-3.

/13/ R. Landauer, "Electrical resistance of disordered onedimensional lattices", *Philosophy Mag.*, V. 21, y. 1970, pp. 863-867.

/14/ M. Büttiker, Y. Imry, R. Landauer, and S. Pinhas, "Generalized many-channel conductance formula with applications to small rings", *Phys. Rev. B*, V. 31, May 1985, pp. 6207-6215.

/15/ R. H. Good Jr. and E. W. Müller, *Handbuch der Physik - Vol. 21*, ed. S. Flugge, Springer, Berlin, 1956, p. 176.

/16/ T. C. L. G. Sollner, *Phys. Rev. Lett.*, V. 59, N. 1622, y. 1987.

/17/ S. Collins, D. Lowe, and J. R. Barker, *J. Appl. Phys.*, V. 63, N. 143, y. 1988.

/18/ F. Chevoir and B. Vinter, *Phys. Rev. B*, **47**, 7260 (1993).

/19/ T. Weil and B. Vinter, *Appl. Phys. Lett.*, **50**, 1281 (1987); S. M. Booker *et al.*, *Semicon. Sci. Technol.*, **7**, B439 (1992).

/20/ H. Yamamoto and X. B. Zhao, Phys. *Stat. Sol. (b)*, **217**, 793 (2000).

/21/ E. O. Kane, *The k × p method - Semiconductors and Semimetals vol. 1*, R. K. Willardson and A. C. Beer, Eds. New York: Academic, 1966, pp. 75-100.

/22/ D. F. Nelson, , R. C. Miller, D. A. Kleinmann, *Phys. Rev. B*, V. 35, y. 1987, pp. 7770.

/23/ U. Merc, F. Smole, and M. Topič, 39th MIDEM Conference Proc., Ptuj, Slovenia, 2003, pp. 213-218.

/24/ S. M. Sze, *Modern Semiconductor Device Physics*, John Wiley & Sons, 1998, ISBN 0-471-15237-4.

/25/ T. Kanagawa, H. Inamoto, T. Kojoima, and K. Ohta, "Observation of resonant tunneling in AlGaAs/GaAs triple barrier diodes", *Appl. Phys. Lett.*, V. 49, July 1986, pp. 73-75.

/26/ H. Mizuta, T. Tanoue, and S. Takahashi, "A new triple-well resonant tunneling diode with controllable double negative resistance", *IEEE Trans. Electron Devices*, V. ED-35, Nov. 1988, pp. 1951-1956.

/27/ C. Pacher, et al., *Appl. Phys. Lett.*, V. 79, N. 10, Sept. 2001, pp. 1486-1488.

/28/ U. Merc et al., Eur. Phys. J. B 35, 443 (2003).

/29/ P. Mazumder, et al., "Digital Circuit Applications of Resonant Tunneling Devices", *Proc. of IEEE*, V. 86, N. 4, April 1998, pp. 664-686.

/30/ A. D. Stone and P. A. Lee, *Phys. Rev. Lett.*, **54**, 1196 (1985); M. Jonson and A. Grincwajg, *Appl. Phys. Lett.*, **51**, 1729 (1987)

Mag. Uroš Merc, Faculty of Electrical Engineering, Tržaška 25, 1000 Ljubljana, Slovenia, +386 (0)1 4768 723, Uros.Merc@fe.uni-lj.si

Mag. Christoph Pacher, ARC Seibersdorf research GmbH, Tech Gate Vienna, Donau-City-Str. 1/4, 1220 Wien, Austria, Christoph.Pacher@arcs.ac.at

Prof. dr. Franc Smole, Faculty of Electrical Engineering, Tržaška 25, 1000 Ljubljana, Slovenia, +386 (0)1 4768 330, Franc.Smole@fe.uni-lj.si

Prof. dr. Marko Topič, Faculty of Electrical Engineering, Tržaška 25, 1000 Ljubljana, Slovenia, +386 (0)1 4768 470, Marko.Topic@fe.uni-lj.si

Prispelo (Arrived): 10.12.2004 Sprejeto (Accepted): 15.03.2005